CHAPTER 1

INTRODUCTION

1.1 Polymer electrolyte membrane (PEM) fuel cell and its development

1.1.1 A basic overview of PEM fuel cell

Recently, throughout the world, the power generation with environmental protection is needed for humanity. Savings in fossil fuels, due to high efficiency of energy conversion, low pollution, and low emissions, are required for development of this novel energy [1, 2].

Fuel cell is an electrochemical engine converter the chemical energy of a fuel as hydrogen and an oxidant as oxygen directly to electrical energy. The primaries products of this engine are water and electricity, thus, it is environmental friendly. During the process, protons are generated and transferred from anode though anode via electrolyte. In other words, proton conductivity is one key step controlling fuel cell performance. Type of fuel cell is classified by its electrolyte that used. Polymer membrane is used for electrolyte of proton exchange membrane fuel cell (PEMFC). It has been approbated as the most promising candidates for application of portable power source, stationary power source, and transportation engine [1-4]. The basic structure of the PEMFC as shown in Figure 1.1 consists of layers of materials which having specific functions. Gases, hydrogen (H_2) and oxygen (O_2) are diffused into the system by gas diffusion layers or GDLs. The membrane, the catalyst layers (CLs), and the two electrodes are assembled

into a sandwich structure which is called membrane-electrode assembly (MEA). PEMFC performance depends on MEA efficiency thus it is a heart of the PEMFC [3, 4].

Since interest in PEMFC research and development has intensified, many researches of PEMFC efficiency improvement have been incessantly reported. Durability, reliability, and cost are mostly considered as particularly significant factors determining PEMFC electric production efficiency. Improvement of stabilized membrane at high temperature was introduced to improve fuel cell durability and reliability [1-5]. To reduce cost, PEMFC with low platinum catalyst loading and alternative catalyst has been developed [3-5].

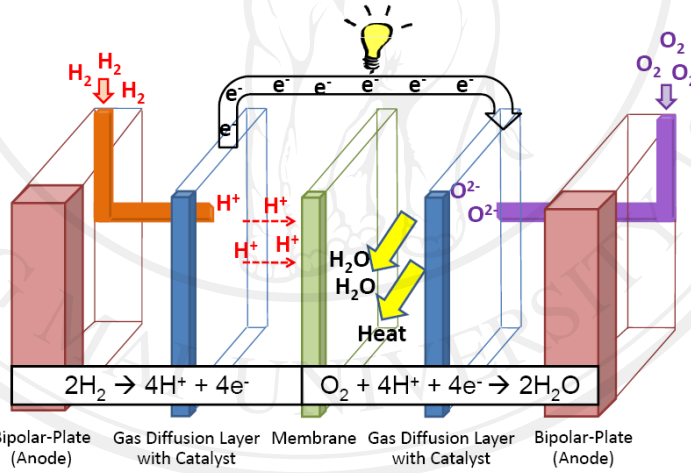

Figure 1.1 Fuel cell working diagram [6]

1.1.2 PEM fuel cell membrane development

As fuel cell membrane is one of crucial parts influencing fuel cell efficiency, numbers of membrane development researches have been studied. Typically, polymer membrane of PEMFC is Nafion® produced by DuPont®, because of its optimized

properties which are high conductivity and thermal durability. It is excellent ionic conductivity when well humidified. Working conductivity range of Nafion is 2 - 5×10^{-2} S cm^{-1}. Its melting point (or loss of cystallinity peaks) is in a range of 207 - 249 °C and glass transition temperature is reported at -108 °C by Starkweather [7] and Corti *et al*. [8]. Two main components of Nafion are the main chain consisting of fluoroethylene units similar to Teflon and the hydrophilic side chain of perfluoro (4-methyl-3,6-dioxa-7octene-1sulfonic acid) or "vinyl ether", as shown in Figure 1.2 [4]. The hydrophilic part is made up of randomly attached long pendant chains terminating with SO_3^-. This part is important for proton diffusion and fuel cell efficiency [9], and lower values of conductivity appear when the number of water per sulfonic group (nH_2O/SO_3H) decrease [10]. Thus, the amount of water which hydrated in Nafion has effect on its proton conductivity efficiency.

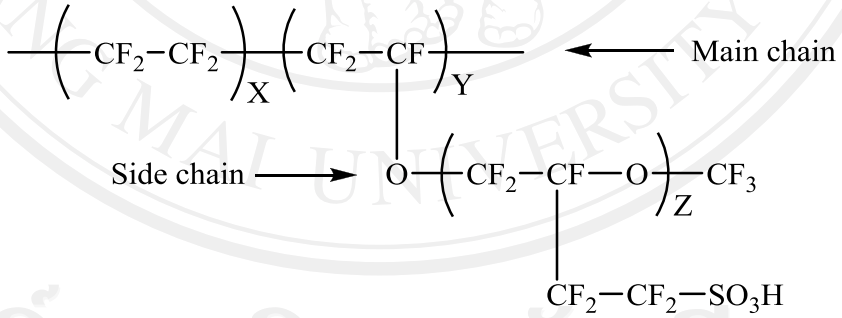

Figure 1.2 The structure of a Nafion polymer [4]

There are several complications of the fuel cell utilization because it must be sufficient water content in the polymer electrolyte, otherwise the conductivity will decrease. This factor effect on cell operations because the moving protons from the anode

to the cathode pull water molecules with them. Furthermore, drying effect of air at high temperatures was accounted and the water balance in the electrolyte must be correct throughout the cell in such case [1, 10]. From above mentioned problem, many researches attempt to improve conducting proton in PEM. By application of composite materials e.g. silica or krytox-silica in Nafion [11-15], proton conductivity of these modified membranes amends because silica composition works as water-absorbent. Moreover, benzimidazole and their derivatives are become potential candidates for water-free proton conducting membrane [16, 17].

Increasing of interface area of electrode and catalyst was studied using ion bombardment on Nafion surface by Cho *et. al*. [5, 18]. The idea is that membrane not only provides ionic conduction pathways between anode and cathode but also acts as a binder for the catalyst particles and these electrodes. Fuel cell performance of treated Nafion by bombardment of argon ion beam was found higher than that was not. Furthermore, platinum loading onto Nafion surface was saved by this modification [5].

1.1.3 Improvement of PEM fuel cell catalyst

To consider catalyst improvement, the slow oxygen reduction reaction (ORR) kinetics on platinum (Pt) catalysts is among the most limiting factors in fuel cell efficiency. Besides, Pt has a high price [19, 20]. Alternative materials are therefore highly sought for fuel cell applications. In fuel cell reduction process, one is production of water through a four-electron pathway, and the other is production of hydrogen peroxide

through a two-electron pathway. The 4 and 2 electron reduction pathways were shown in equation (1.1) and (1.2) respectively [20].

$$O_2 + 4H^+ + 4e^- \rightarrow 2H_2O \quad (1.1)$$

$$O_2 + 2H^+ + 2e^- \rightarrow H_2O_2 \quad (1.2)$$

However, the harmful anode material can be gotten if the 2 electron pathway occurred in acidic condition of H_2O_2 product. As Pt catalyzed cathode oxygen reduction is not a complete 4 electron reaction [21], therefore, the improvement of ORR catalyst should base on (i) high activity, (ii) low cost, and (iii) encouragement of 4 electron pathways. In order to reduce the cost of the fuel cell catalysts, two approaches are currently very active: exploration of non-noble metal catalysts, and reduction of Pt loading. Non-noble metal catalyst, metal pyridine such as Fe-N_X/C, deposited Fe which has N as the ligand is one of employer [20, 22, 23]. In Fe-N_X/C catalytic sites, most possible structures of Fe-N_X/C are Fe-N_4/C and Fe-N_2/C as shown in Figure 1.3 [22]. In the reduction of Pt loading, plasma sputtering deposition of Pt dope on carbon support such as graphite was attempted [3].

Fe-N_4/C Fe-N_2/C

Figure 1.3 Most possible structure of Fe-N_X/C [22]

As fuel cell is alternative energy engine and environmental friendly technology, thus it has benefit for humanity. Recently, acquisition of fundamental knowledge is talented to develop fuel cell performance. For example, improvement efficiencies of membrane and alternative catalyst of ORR, however, these phenomena are not well understood, in particular, at atomistic level. The substantially understanding will be benefit for further fuel cell development.

1.2 Computational studies in PEM fuel cell materials

The geometry of Nafion side chain had been investigated by Paddison and Zawodzinski [24] through trifluoromethane sulfonic acid fragment (CF_3SO_3H), the di-trifluoromethane ether fragment (CF_3OCF_3), and the side chain (CF_3-$OCF_2CF(CF_3)$ $OCF_2CF_2SO_3H$). Several rotational potential energy surfaces were calculated to assess chain flexibility and proton accessibility. Molecular dynamics simulations were performed and the results indicated that although the side chain with sulfonate group is rather flexible, the shape of curled up structure obtained from optimization is quite stable.

Molecular modeling simulation has been used to understand the crucial actions in proton transfer process. Elliott *et al*. [25] studied an atomistic model for PIMs in particular Nafion materials. They found that the electrostatic term in the Dreiding II force field is responsible for the formation of an apparently phase separated morphology which is selectively conductive, favouring the passage of cations. The H_3O^+ mobility is shown to be consistent with a jump diffusion model of ion transport in PIMs. There is

also evidence for the existence of water in two distinct environments in the simulations: both tightly bound to ion exchange groups, and more loosely associated with the fluorocarbon matrix. *Ab initio* molecular dynamics calculations were performed to explore the defect structure for proton transport in a triflic acid of perfluorosulfonic acid monohydrate crystal [26] by Eikerling *et al*. [27]. They pointed out that the proton was transferred by Zundel ion, forming of one water molecule bond with one H_3O^+. In addition, aqueous pore structure and proton dynamics in solvated Nafion membranes resulted in characteristic differences in aqueous pore structure was studied by Seeliger *et al*. [28]. These were observed for systems whose water content was varied between 5 and 10 molecules per acid group in the polymer. As expected, proton transport increases significantly with increasing humidity. Its mechanism is dominated by the Grotthus structural diffusion mechanism in accordance with earlier studies in simplified pores model. On the simulated time scale, no unambiguous conclusions on the role of polymer dynamics for the transport in dry membranes can be drawn. Additionally, to observe the water molecules penetrate a silica film through a proton-transfer process which is similar to the Grotthuss mechanism, hydrogen hopping was studied by MD simulation in Fogarty *et al*. work [29]. Hydrogen atoms pass through the film by associating and dissociating with oxygen atoms within bulk silica, as opposed to diffusion of intact water molecules.

To concern alternative material aspect, heterocyclic such as imidazole and pyrazole are promising in this respect. Their basic nitrogen sites act as strong proton acceptors with respect to the sulfonic acid group thus forming protonic charge carriers

$(C_3H_3NH_2)^+$. Its higher temperature stability and imidazole (pyrazole), a stronger Bronstedt base compared to water, was projected to be useful for the application of materials as fuel cell electrolyte. Kreuer *et al*. [30] studied the imidazole and pyrazole-based proton conducting polymer and liquids. They found that the creation of protonic defects and the mobility of protons in these environments were found to be similar to the situation in corresponding water containing system. Moreover, Herz *et al*. [31] studied a new fully polymer proton solvents with high proton mobility. They prepared two different types of polymer, polystyrene with imidazole terminated flexible side chains and benzimidazole covalently bonded to an inorganic SiO_2 network by a flexible spacer. They found that high proton conductivities of up to 7×10^{-4} S cm^{-1} at 200°C have been obtained for these polymers in the absence of water and this conductivity value corresponding to a high mobility of protonic charge carriers.

To simulate surface change from ion bombardment at a high energy range, Fekete *et al*. [32] modeled the effects of ion implantation into Nafion, using MC simulation [32]. In this visual study, a selected series of the positive ions with energies of 20-320 keV, were used to bombard the target polymer. They found that the ion energies of 100-200 keV can affect the outer 0.5-3 μm of the surface layer. The depth of the implanted ions in Nafion increases as the ion energies increased. Additionally, the collisions between ions and polymer moiety can alter the permeability of the Nafion membrane. The MD simulation technique can applies for the studies of the modification of synthetic and natural polymers by atom/ion bombardment [33-35]. Végh *et al*. [33] reported that the MD results by repeated impact in order to mimic

higher ion doses can exhibit a formation of a heavily cross-linked and dehydrogenated damaged layer of polystyrene model. Also, sputtering yield of carbon after bombardment analyzed in terms of the ratio of carbon per Ar^+ is consistent with the observed experiment. Sinnott *et. al*. [34] studied of the MD simulations of modification of poly(methyl methacrylate) or PMMA surface by 1 keV Ar atom bombardment. They indicated that the deposition of Ar atoms on PMMA produces chemical changes within the PMMA substrate and etches the surface. Another example is that the low energy ion bombardment on naked DNA was studied using MD simulations [35]. They proposed a useful technique for analysis of bond-breaking occurring in nucleotides. Also, changes in bond lengths and visibly distorted structures of bombarded nucleotides were clearly observed from the MD results.

1.3 Theoretical Methodologies and Simulation Tools

Quantum chemistry is based on quantum mechanical principles, defined by the mathematical descriptions of chemistry. A wavefunction obtained by solving of *Schrödinger equation* [36], is the tool of quantum chemistry for describing the properties of matter in terms of energies and positions of the nuclei and electrons. However, only simple chemical systems can be determined through the purely quantum chemistry terms. For complicated systems, the simplification of quantum mechanics, such as Hartree-Fock (HF) or density functional theory (DFT), are mostly applied for the convenient investigations.

1.3.1 Schrödinger equation

The complete description of a wavefunction can be given through the solution of the Schrödinger equation, which describing the atom system. Schrödinger obtained an equation by taking the classical time-independent wavefunction equation.

$$[-(h^2/8\pi^2 m)\nabla^2 + V(x,y,z)\psi(x,y,z)] = E\psi(x,y,z), \quad (1.3)$$

Equation (3) represents the *Schrödinger's time-independent* wave equation for a single particle of the mass (m) moving in the three-dimensional potential field (V). The left-hand side of the equation is called the *Hamiltonian operator* (H),

$$H \equiv -(h^2/8\pi^2 m)\nabla^2 + V, \quad (1.4)$$

which is often written as

$$H\psi = E\psi. \quad (1.5)$$

The Hamiltonian operator takes into account five contributions to the total energy of the system, namely the kinetic energies of the electrons and nuclei, the attraction of the electrons to the nuclei and the interelectronic and internuclear repulsions that would be of the form

$$H = -\sum_i \frac{\hbar^2}{2m_e}\nabla_i^2 - \sum_k \frac{\hbar^2}{2m_k}\nabla_k^2 - \sum_i \sum_k \frac{e^2 Z_k}{r_{ik}} + \sum_{i<j} \frac{e^2}{r_{ij}} + \sum_{k<l} \frac{e^2 Z_k Z_l}{r_{kl}}, \quad (1.6)$$

where i and j defined to electrons, k and l run over nuclei, $\hbar$ is *Plank's constant* divided by 2π, m_e is the mass of the electron, m_k is the mass of nucleus, e is the electron charge, Z is an atomic number, r_{ab} is the distance between particles a and b and ∇^2 is the *Laplacian operator*, which can be defined as

$$\nabla^2 \equiv \frac{\partial^2}{\partial x^2} + \frac{\partial^2}{\partial y^2} + \frac{\partial^2}{\partial z^2}. \tag{1.7}$$

1.3.2 Born-Oppenheimer approximation

The difficulty for solving the Schrödinger equation appears in the many-particle molecular systems involving correlated motions of particles. In fact, the nuclei are heavier than electrons, thus, the nuclei are moving slowly than the electrons. According to this property, the approximation has been made by separating the nuclei and electrons motions, called *Born-Oppenheimer approximation*.

Based on Born-Oppenheimer approximation, the electronic energies are computed by fixing nuclear position. Consequently, the nuclear kinetic energy term is independent, and thus, can be neglected. The attractive electron-nuclear potential energy term is eliminated and the repulsive nuclear-nuclear potential energy term can be considered to be constant. Thus, the electronic Schrödinger equation can be defined as

$$(H_{el} + V_N)\Psi_{el}(q_i; q_k) = E_{el}\Psi_{el}(q_i; q_k), \tag{1.8}$$

where the subscript *el* refer to the Born-Oppenheimer approximation, H_{el} includes only the first, third and fourth terms on the equation (1.6) as

$$H_{el} = -\sum_i \frac{\hbar^2}{2m_e}\nabla_i^2 - \sum_i \sum_k \frac{e^2 Z_k}{r_{ik}} + \sum_{i<j} \frac{e^2}{r_{ij}}, \tag{1.9}$$

where V_N is the nuclear-nuclear repulsion energy, q_i is the electronic coordinates and q_k is the nuclear coordinates. The eigenvalue of the electronic Schrödinger equation is called the *electronic energy* (E_{el}). Since the term V_N is a constant for a given set of fixed

nuclear coordinates, the wavefunction can be solved without the inclusion of V_N. In this respect, the eigenvalue is called the *pure electronic energy*. The term V_N can be added to this eigenvalue in order to obtain the total electronic and nuclear-nuclear repulsion energy.

1.3.3 Molecular orbital theory

The molecular orbital theory is a method for determining molecular structure. A molecular orbital is a region in which an electron may be found in a molecule. The molecular orbital can be described by the wavefunction of the electron in a molecule, in particular a spatial distribution ($|\psi_i(r)|^2$) of an electron and energy of up to two electrons within it. The complete wavefunction for an electron is consist of a molecular orbital and a spin function (α and β), which can be defined as a *spin orbital* ($\chi(x)$) where *x* indicates both space and spin coordinates. Therefore, a spatial orbital can be formed into two different spin orbitals as

$$\chi(x) = \begin{cases} \psi(r)\alpha(\omega) \\ \psi(r)\beta(\omega). \end{cases} \tag{1.10}$$

For *N*-electron wavefunction, the Hamiltonian of the simpler system, which contained noninteracting electrons, can be defined as

$$H = \sum_{i=1}^{N} h(i), \tag{1.11}$$

where *h(i)* is the operator that describes the kinetic energy and potential energy of electron *i*. Then, the set of spin orbitals ($\chi_j(x)$) have been added to the operator, which presented in equation (1.12),

$$h(i)\chi_j(x_i) = \varepsilon_j \chi_j(x_i). \tag{1.12}$$

Therefore, the wavefunction is a simple product of spin orbital wavefunction for each electron as

$$\Psi^{HP}(x_1, x_2, ..., x_N) = \chi_i(x_1)\chi_j(x_2)\cdots\chi_k(x_N). \tag{1.13}$$

Thus, the equation (1.5) can be written as

$$H\Psi^{HP} = E\Psi^{HP}, \tag{1.14}$$

where *E* is the sum of the spin orbital energies of each spin orbital in Ψ^{HP}, as

$$E = \varepsilon_i + \varepsilon_j + \cdots + \varepsilon_k. \tag{1.15}$$

Accordingly, a *N*-electron wavefunction is termed a *Hartree product*, where the electron-one has been described by the spin orbital (χ_i), electron-two has been described by the spin orbital (χ_j), etc. However, this wavefunction does not allow the antisymmetry principle.

To satisfy correcting the antisymmetry principle, considering a two-electron case in order to put electron-one in χ_i and electron-two in χ_j as

$$\Psi_{12}^{HP}(x_1, x_2) = \chi_i(x_1)\chi_j(x_2). \tag{1.16}$$

In the opposite way, putting electron-one in χ_j and electron-two in χ_i as

$$\Psi_{21}^{HP}(x_1, x_2) = \chi_i(x_2)\chi_j(x_1). \tag{1.17}$$

After that, taking the appropriate linear combination of these two Hartree products,

$$\Psi(x_1, x_2) = 2^{-1/2}(\chi_i(x_1)\chi_j(x_2) - \chi_i(x_2)\chi_j(x_1)), \tag{1.18}$$

where the factor $2^{-1/2}$ is a normalization factor and the minus sign insures that $\Psi(x_1, x_2)$ is antisymmetric with respect to the interchange of the coordinates of electrons one and two. From equation (1.18), the wavefunction disappears if both electrons occupy the same spin orbital, *i.e.*, following the *Pauli exclusion principle*. Moreover, the antisymmetric wavefunction can be rewritten in terms of a determinant,

$$\Psi(x_1, x_2) = 2^{-1/2}\begin{vmatrix} \chi_i(x_1) & \chi_j(x_1) \\ \chi_i(x_2) & \chi_j(x_2) \end{vmatrix}, \tag{1.19}$$

which is called a *Slater determinant* [37]. For an *N*-electron system, the generalization is

$$\Psi(x_1, x_2, ..., x_N) = (N!)^{-1/2}\begin{vmatrix} \chi_i(x_1) & \chi_j(x_1) & \cdots & \chi_k(x_1) \\ \chi_i(x_2) & \chi_j(x_2) & \cdots & \chi_k(x_2) \\ \vdots & \vdots & \ddots & \vdots \\ \chi_i(x_N) & \chi_j(x_N) & \cdots & \chi_k(x_N) \end{vmatrix}, \tag{1.20}$$

where the factor $(N!)^{-1/2}$ is the normalization factor.

1.3.4 The LCAO approach and basis sets

The molecular orbitals can be built from the atomic orbitals by using the *linear combination of atomic orbitals to molecular orbitals* (LCAO-MO) method. The relation can be written as

$$\psi_i = \sum_{\mu=1}^{N} C_{\mu i}\phi_\mu, \tag{1.21}$$

where $C_{\mu i}$ are the molecular orbital expansion coefficients, *N* is the number of atomic basis function and the set of *N* function ϕ_{μ} is called *basis set*.

The common types of basis function, as also called *atomic orbital*, used in electronic structure calculations are *Slater-type orbitals* (STOs) [38] and *Gaussian-type orbitals* (GTOs) [39].

For the STOs, they are constructed as

$$\psi(n,l,m_l;r,\theta,\phi) = Nr^{n_{eff}-1}e^{-Z_{eff}\rho/n_{eff}}Y_{lm_l}(\theta,\phi), \qquad (1.22)$$

where *n, l,* and m_l are the quantum numbers, *N* is the normalization constant and Y_{lm_l} is a spherical harmonic. The exponential dependence on the distance between the nucleus and electron mirrors the exact orbitals for the hydrogen atom, where Z_{eff} is the effective nuclear charge in which the effective principal quantum number (n_{eff}) is related to the true principal quantum (n) by the following mapping as

$$n \to n_{eff} : 1 \to 1 \quad 2 \to 2 \quad 3 \to 3 \quad 4 \to 3.7 \quad 5 \to 4.0 \quad 6 \to 4.2,$$

and the value of ρ equal to r/a_0, where a_0 is *Bohr radius*.

The STOs are usually applied for atomic and diatomic systems, which high accuracy, as well as in semi-empirical methods, where all three- and four-center integrals are neglected. In density functional methods, exact exchange is not included and the coulomb energy is calculated by fitting the density to a set of auxiliary functions. However, the STOs do not satisfy in two-electron integral problem. The feasible basis function is GTOs, which are function of the form

$$\theta_{ijk}(r_1 - r_c) = (x_1 - x_c)^i (y_1 - y_c)^j (z_1 - z_c)^k e^{-\alpha|r_1 - r_c|^2}, \qquad (1.23)$$

where (x_c, y_c, z_c) are the Cartesian coordinates of the center of the Gaussian function at r_c , (x_1, y_1, z_1) are the Cartesian coordinates of an electron at r_1, i, j and k are non-negative integers and α is a positive exponent. The advantage of GTOs is that the product of two Gaussians at different centers is equivalent to a single Gaussian function centered at a point between the two centers. Therefore, the two-electron integral problem on three and four or more different atomic centers can be reduced to integrals over two different centers.

The most important factor for creating the molecular orbital is the set of parameters when applied to the basis function, called *basis set*. The smallest number of function possible is a *minimum basis set*. The improvement of the basis set can be achieved by replacing two basis functions into each basis function in the minimal basis set, called *double zeta* (DZ). Accordingly, a *triple zeta* (TZ) refers to three basis functions that are used to represent each of the minimal basis sets. The compromise between the DZ and TZ basis sets is called a *split valence* (SV) basis set, in which each valence atomic orbital is represented by two basis functions whereas each core orbital is represented by a single basis function.

1.3.5 Hartree-Fock method

The important factor in the electronic structure calculations is the electron-electron repulsions, which must be included in any accurate electronic structure treatment. The *Hartree-Fock* (HF) method treats the electron-electron repulsions in an

average way. The HF equation for spin orbital (ϕ_a), which assigning electron 1 to spin orbital (ϕ_a), is

$$f_1\phi_a(1) = \varepsilon_a\phi_a(1), \tag{1.24}$$

where ε_a is the spin orbital energy and f_1 is the *Fock operator*. The f_1 can be defined as

$$f_1 = h_1 + \sum_u \{J_u(1) - K_u(1)\}, \tag{1.25}$$

where h_1 is the core Hamiltonian for electron 1, the sum is over all spin orbital $u = a,b,\ldots,z$, J_u is the Coulomb operator and K_u is the exchange operator. The J_u and K_u operator can be defined as

$$J_u(1)\phi_a(1) = j_0\left\{\int \phi_u^*(2)\frac{1}{r_{12}}\phi_u(2)dx_2\right\}\phi_a(1), \tag{1.26}$$

$$K_u(1)\phi_a(1) = j_0\left\{\int \phi_u^*(2)\frac{1}{r_{12}}\phi_a(2)dx_2\right\}\phi_u(1), \tag{1.27}$$

where j_0 is $\frac{e^2}{4\pi\varepsilon_0}$.

The Coulomb operator takes into account the coulombic repulsion and the exchange operator represents the modification of this energy that can be ascribed to the effect of spin correlation. In equation (1.25), the sum represents the average potential energy of electron 1 due to the presence of the other n-1 electrons. Since the Fock operator depends on the spin orbitals of all the other n-1 electrons, the HF method must already know the solution beforehand, thus, the iterative style of solution has been carried

out and stopping when the solution is self-consistent, as called *self-consistent field* (SCF). The self-consistent is started with a trial set of spin orbitals and used to construct the Fock operator. After that, the HF equation is solved to obtain the new set of spin orbitals, which are used to construct a revised Fock operator, and so on. The calculation is repeated until a convergence criterion is satisfied.

In general, the SCF calculation produces the different energy value, depending on the basis set. For example, using a minimal basis set yields a total electronic energy E1. The energy E1 can be improved by choosing a new basis set like a double zeta basis, *i.e.*, to compute the lower energy E2. Moreover, the polarization function can be added into the basis set to give the lower energy E3. On the other hand, the expansion of the basis set will decrease the total electronic energy. Nevertheless, since the basis sets used in the calculations are finite, thus, the energy will approach a limiting value. This limiting energy is called a *Hartree-Fock limit*. The molecular orbitals that correspond to this limit are called *Hartree-Fock orbitals* (HF orbitals) and the determinant is called the HF wavefunction.

1.3.6 Density functional theory

For the treatment of system containing many atoms and many electrons, the *ab initio* methods are found to be very time-consuming. The *density functional theory* (DFT) is then used as an alternative approach, which takes into account the electron correlation using the concept of electron probability density. The energy of an electronic system is described in terms of the electron probability (ρ). In many electrons system, the total

electron density at a particular point *r* in space can be denoted as ρ(r). The electronic energy (*E*) is the functional of the electron density, which can be defined as $E(\rho)$.

The DFT method considers the pair electrons in the same spatial one-electron orbitals. Kohn and Sham suggest that the exact ground-state electronic energy (*E*) of an *n*-electrons system can be of the form

$$E(\rho) = -\frac{\hbar_2}{2m_e}\sum_{i=1}^{n}\int \psi_i^*(r_1)\nabla_1^2\psi_i(r_1)dr_1 - j_0\sum_{I=1}^{N}\frac{Z_I}{r_{I1}}\rho(r_1)dr_1$$

$$+\frac{1}{2}j_0\int\frac{\rho(r_1)\rho(r_2)}{r_{12}}dr_1dr_2 + E_{\mathrm{XC}}[\rho]. \qquad (1.28)$$

The first term of equation (1.28) describes the kinetic energy of the electron. The second term represents the electron-nucleus attraction in which the sum is over all *N* nuclei with index *I* and atomic number Z_I. The third term refers to the Coulumb interaction between the total charge distribution at r_1 and r_2 and the last term is the *exchange-correlation energy* of the system. The one-electron spatial orbitals (ψ_i; i = 1, 2, …, n) are the *Kohn-Sham* (KS) [39] orbital. The exact ground-state electron density can be defined by

$$\rho(r) = \sum_{i=1}^{n}|\psi_i(r)|^2. \qquad (1.29)$$

The KS orbital can be described by solving the *Kohn-Sham* [39] equation and the one-electron orbital ($\psi_i(r_1)$) can be of the form

$$\left\{-\frac{\hbar^2}{2m_e}\nabla_1^2 - j_0\sum_{I=1}^{N}\frac{Z_I}{r_{I1}} + j_0\int\frac{\rho(r_2)}{r_{12}}dr_2 + V_{\mathrm{XC}}(r_1)\right\}\psi_i(r_1) = \varepsilon_i\psi_i(r_1), \qquad (1.30)$$

where ε_i are the KS orbital energies and V_{XC} is the exchange-correlation potential, which can be derived from the exchange-correlation energy,

$$V_{XC}[\rho] = \frac{\delta E_{XC}[\rho]}{\delta \rho}. \tag{1.31}$$

Starting with the guess electron density (ρ), a self-consistent fashion is employed for calculating the KS equations. By using an appropriate form of the $E_{XC}[\rho]$, the V_{XC} can be calculated as the function of *r*. The set of KS equation is solved in order to obtain an initial set of KS orbitals. Then, the set of orbitals is used to compute an improved density from equation (1.29). These procedures reach convergence when the density and exchange-correlation energy are satisfied.

According to the calculation process, the main error of DFT is the approximation of $E_{XC}[\rho]$. This function can be separated into an exchange functional and a correlation function. In the *local density approximation* (LDA), the exchange-correlation can be defined as

$$E_{XC} = \int \rho(r)\varepsilon_{XC}[\rho(r)]dr, \tag{1.32}$$

where $\varepsilon_{XC}[\rho(r)]$ is the exchange-correlation energy per electron in a homogeneous electron gas of constant density.

To improve the exchange-correlation function, a non-local correction involving the gradient of ρ is added to the exchange-correlation energy. The LDA with gradient-corrections is called the *generalized gradient approximation* (GGA). The exchange-correlation functionals have been developed for use in DFT calculations, such as mPWPW91, B3LYP, MPW1K, PBE1PBE, BLYP, BP91 and PBE. The name of each function refers to the pairing of an exchange function and correlation function. For example, the BLYP function is a combination of the gradient-corrected exchange

functional, developed by Becke [40,41], and the gradient-corrected correlation functional developed by Lee, Yang and Parr [42]. The B3LYP function makes use of Hartree-Fock corrections in conjunction with density function correlation and exchange. Nowadays, the DFT calculations are widely used for large molecular systems, such as protein.

1.3.7 Molecular mechanics

The molecular mechanics (MM) or force field method use *classical mechanics* models to predict the energy of a molecule as a function of its conformation. The molecule is treated at the atomic level by capture very simple interactions between atoms but the electrons are not treated explicitly. A force field function is a rather simple model of the interactions within a system with contributions from processes such as the stretching of bonds, the opening and closing of angles and rotations about single bonds. Even when simple functions (e.g. Hooke's law) are used to describe these contributions, the force field can perform quite acceptably. Transferability is a key attribute of a force field, for it enables a set of parameters developed and tested on a relatively small number of cases to be applied to a much wider range of problems. Moreover, parameters developed from data on small molecules can be used to study much larger molecules such as polymers.

1.3.7.1 Energy function

Many of the energy function or force fields function in use today for molecular systems can be interpreted in terms of a relatively simple five component

picture of the intra- and intermolecular forces within the system. Energetic penalties are associated with the deviation of bonds and angles away from their 'reference' or 'equilibrium' values. One functional form of a simple force field that can be used to model single molecules or assemblies of atoms and/or molecules is

$$E_{Total} = E_{bonds} + E_{angle} + E_{dihe} + E_{vdw} + E_{elec} \tag{1.33}$$

Where E_{Total} is the total energy of a system, E_{bonds} is the interaction between two atoms directly bonded to each other, E_{angle} is the interaction between three connected atoms, E_{dihe} is the energies associated with dihedral angles, E_{vdw} is the balance of the attractive at long range (due to London, Dispersion forces), but are strongly repulsive at short range and E_{elec} is the electrostatics interaction. Each function in Equation (1.33) is defined as the following:

$$E_{bonds} = \sum_{bonds} k_b (b - b_0)^2 \tag{1.34}$$

$$E_{angle} = \sum_{angle} k_\theta (\theta - \theta_0)^2 \tag{1.35}$$

$$E_{dihe} = \sum_{dihe} k_\chi (1 + (\cos(n\chi - \delta)) \tag{1.36}$$

$$E_{vdw} = \sum_{nonbond} \varepsilon_{ij} \left[\left(\frac{R_{\min,ij}}{r_{ij}} \right)^{12} - 2 \left(\frac{R_{\min,ij}}{r_{ij}} \right)^{6} \right] \tag{1.37}$$

$$E_{elec} = \sum_{nonbond} \frac{q_i q_j}{4\pi\varepsilon_0 r_{ij}} \tag{1.38}$$

Where $k_b, k_{\theta,} k_{\chi}$ are the force constants of bond stretching, bending and dihedral, respectively. The $b_o, \theta_{o,} \delta$ symbols are the reference values of the bond, angle and dihedral angle, respectively.

More sophisticated force fields may have additional terms as cross terms, but they invariably contain these five components. An attractive feature of this representation is that the various terms can be ascribed to changes in specific internal coordinates such as bond lengths, angles, rotation of bonds or movements of atoms relative to each other.

1.3.7.2 Force field parameterization

Force field parameterization is quite difficult and computationally intensive. A set of parameters of a force field function has to fit to structures (and properties) for a training set of molecules. The *ab initio* data at minima and distorted geometries or experimental values of the selected molecules can be used for trial and error fit. The quality and reliability of the fitted parameters for a force filed function have to check and test before use or apply for other systems.

1.3.7.3 COMPASS force field

The COMPASS force field, a powerful force field that supports atomistic simulations of polymers, was used for all calculations [43,44]. The potentials function of COMPASS force field was shown in equation 1.39 [44]. The functions are divided into two categories, bonded and nonbonded terms. Bond (b), angle (θ), torsion angle (ϕ), and the cross-coupling terms include combinations of two or three internal coordinates are

represented for bonded term. The LJ-9-6 function used for the van der Waals (vdW) term and a Coulombic function used for an electrostatic interaction are represented for nonbonded interaction term.

$$
\begin{aligned}
E_{total} = & \sum_{b}[k_2(b-b_0)^2 + k_3(b-b_0)^3 + k_4(b-b_0)^4] \\
& + \sum_{\theta}[k_2(\theta-\theta_0)^2 + k_3(\theta-\theta_0)^3 + k_4(\theta-\theta b_0)^4] \\
& + \sum_{\phi}[k_1(1-\cos\phi) + k_2(1-\cos 2\phi) + k_3(1-\cos 3\phi)] \\
& + \sum_{\chi} k_2\chi^2 + \sum_{b,b'} k(b-b_0)(b'-b_0') + \sum_{b,\theta} k(b-b_0)(\theta-\theta_0) \\
& + \sum_{b,\phi}(b-b_0)[k_1\cos\phi + k_2\cos 2\phi + k_3\cos 3\phi] \\
& + \sum_{\theta,\phi}(\theta-\theta_0)[k_1\cos\phi + k_2\cos 2\phi + k_3\cos 3\phi] + \sum_{b,\theta} k(\theta'-\theta_0')(\theta-\theta_0) \\
& + \sum_{\theta,\theta,\phi} k(\theta-\theta_0)(\theta'-\theta_0')\cos\phi + \sum_{ij}\frac{q_i q_j}{r_{ij}} + \sum_{ij}\epsilon_{ij}\left[2\left(\frac{r_{ij}^{\,0}}{r_{ij}}\right)^9 - 3\left(\frac{r_{ij}^{\,0}}{r_{ij}}\right)^6\right]
\end{aligned}
\tag{1.39}
$$

1.3.7.4 Energy minimization

Optimization is a general term for finding stationary points of a function. In the majority of cases, the desired stationary point is a minimum (points where the first derivative is zero & all the 2nd derivatives are positive). In some cases, the desired point is a first-order saddle point (the 2nd derivative is negative in one, and positive in all other, directions. Optimization to minima is also referred to as energy minimization in which it depends on computational method you use. It is a series of iterations (process is repeated) performed on the molecule until the energy of the molecule has reached a minimum. All commonly used methods assume that at least the 1st derivative of the function with respect to all variables, the gradient (g), can be calculated analytically. There are mostly

used techniques in energy minimization that are steepest descent (SD), conjugated gradient (CG) and Newton-Raphson method.

1.3.8 Molecular dynamic simulations

In terms of computation simulations, the molecular dynamics (MD) technique is well-known. This technique is widely used for studying various molecular systems. MD simulation provides the time dependent behavior of a molecular system. The MD simulation starts with reading in the initial configuration, such as coordinates, velocities, accelerations and forces. The initial configuration can be obtained from random configurations or a lattice. One of the essential conditions of the simulation is that there are no explicitly time-dependent or velocity dependent forces that shall act on the system. In practice, the trajectories cannot be directly obtained from Newton's equation. Therefore, the *time integration algorithm* will be used to obtain the knowledge of positions, velocities and accelerations of two successive time steps. The energy of the system can be calculated using molecular mechanics (MM) or quantum mechanics (QM) methods. The force on each atom can be obtained from the derivative of the energy with respect to the change in the atom's position. The particles will be moved by their new force to the new configurations. This process will be repeated until the system reaches equilibrium. Then, the coordinates, velocities, accelerations, forces and so on of all particles will be collected for further structural and dynamical property calculations. In most cases, only positions and velocities are usually stored since most important

properties can be obtained from these two quantities. The schematic of molecular dynamics simulation is shown in Figure 1.4

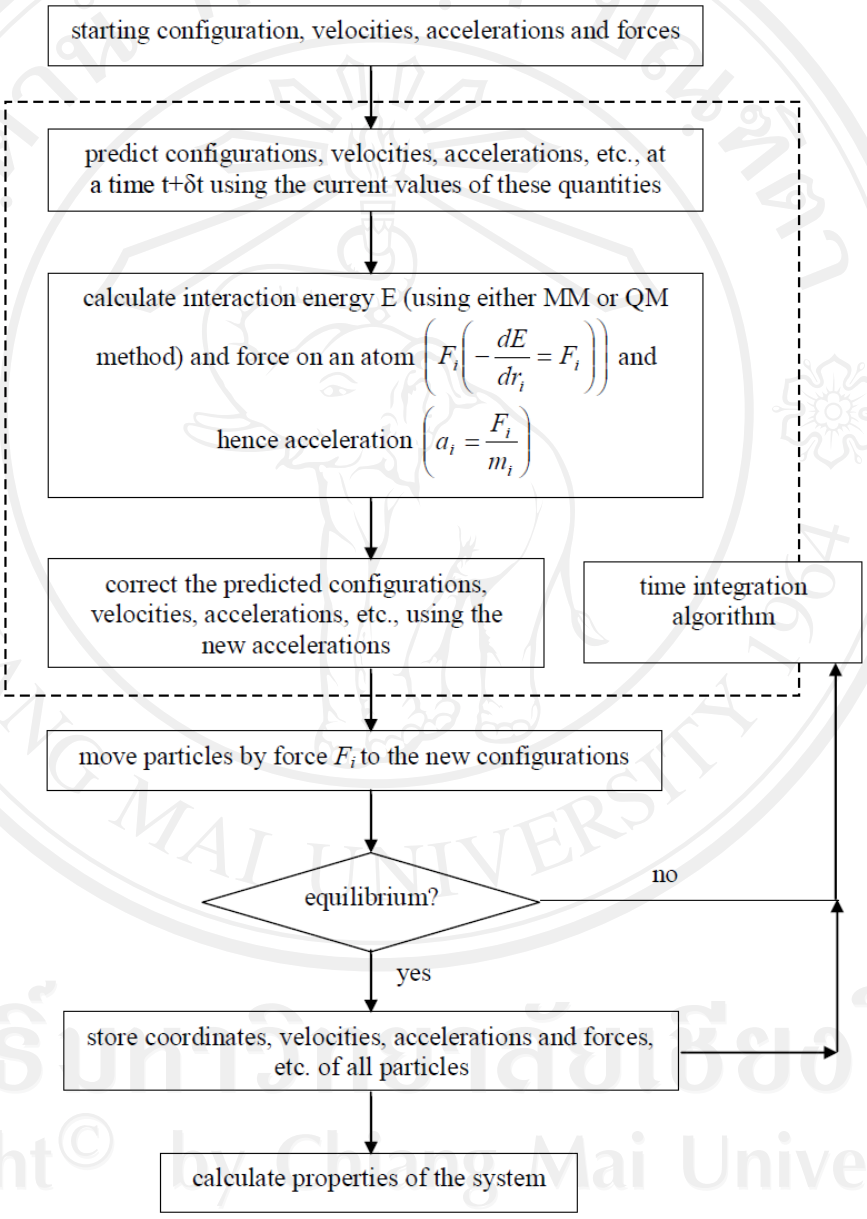

Figure 1.4 The schematic of molecular dynamics simulation

1.3.8.1 Time average and ensemble average

The properties of the system will depend upon the positions and the momenta of *N* particles that comprise the system. The value of the property *A* can thus be written as

$$A(\mathrm{p}^N(t), \mathrm{r}^N(t)), \tag{1.40}$$

where $\mathrm{p}^N(t)$ and $\mathrm{r}^N(t)$ represent the *N* momenta and positions, respectively. The value of property *A* is the average of the *A* over the time of the measurement, known as a *time average*. In principle, if the time measurement reach infinity, the value of the property *A* is then the *true value*,

$$A_{ave} = \lim_{\tau\to\infty} \frac{1}{\tau} \int_{t=0}^{\tau} A(\mathrm{p}^N(t), \mathrm{r}^N(t))dt. \tag{1.41}$$

In practice, the treatment for system consisting of a large number of atoms or molecules is not feasible, even the determination of an initial configuration of the system. Boltzmann and Gibbs developed statistical mechanics, known as *ensemble*. The ensemble is a single system evolving in time that contains a large number of mental copies of a system, considered all at once, each of which represents a possible state of the real system. The time average is then replaced by an *ensemble average* as

$$\langle A \rangle = \iint d\mathrm{p}^N d\mathrm{r}^N A(\mathrm{p}^N, \mathrm{r}^N)\rho(\mathrm{r}^N, \mathrm{r}^N). \tag{1.42}$$

The angle bracket (< >) indicates an ensemble average or *expectation value*, *i.e.*, the average value of the property *A* over all replications of the ensemble generated by the simulation. Different macroscopic environmental constraints lead to different types of ensembles. In general, the ensemble is employed with constraints, such as constant number of particles (N), volume (V), energy (E), temperature (T), chemical potential (μ),

pressure (P) and so on. For example, the *microcanonical ensemble* (NVE) fixes the number of particles (N), the volume (V) and the energy (E) of the system. The equilibrium states of NVE ensemble characterize the entropy. Another example is the *canonical ensemble* (NVT), which fixes the number of particles (N), the volume (V) and the temperature (T). The thermodynamic property derived from the NVT ensemble is Helmholtz free energy. Other ensembles include the *grand canonical ensemble* (μVT), which fixes the chemical potential (μ), the volume of the system (V) and the temperature (T). The pressure×volume (PV) quantity can be obtained from this ensemble.

1.3.8.2 Time-integration algorithms

In general, there are many algorithms for integrating the equations of motion, most of which are based on *finite difference method*. By this method, the integration is broken down into many small stages, each separated in time by a fixed time interval Δt. The total force on each particle in the system at time t is calculated as the vector sum of its interactions with other particles. Then, the positions and velocities at a time t are used to calculate the positions and velocities at a time $t + \Delta t$. Then, the new positions and velocities have been calculated at time $t + 2\Delta t$, and so on.

All algorithms assume that the positions and dynamic properties can be approximated as *Taylor series expansion*,

$$\mathrm{r}(t + \Delta t) = \mathrm{r}(t) + \Delta t \mathrm{v}(t) + \frac{1}{2}\Delta t^2 \mathrm{a}(t) + \frac{1}{6}\Delta t^3 \mathrm{b}(t) + \frac{1}{24}\Delta t^4 \mathrm{c}(t) + \cdots, \quad (1.43)$$

$$\mathrm{v}(t + \Delta t) = \mathrm{v}(t) + \Delta t \mathrm{a}(t) + \frac{1}{2}\Delta t^2 \mathrm{b}(t) + \frac{1}{6}\Delta t^3 \mathrm{c}(t) + \cdots, \quad (1.44)$$

$$\mathrm{a}(t+\Delta t) = \mathrm{a}(t) + \Delta t\mathrm{b}(t) + \frac{1}{2}\Delta t^2\mathrm{c}(t) + \cdots, \tag{1.45}$$

$$\mathrm{b}(t+\Delta t) = \mathrm{b}(t) + \Delta t\mathrm{c}(t) + \cdots. \tag{1.46}$$

The first derivative of the position (r) with respect to time is the velocity (v), the second derivative is the acceleration (a) and the third derivative is b, and so on. The widely used methods for integrating the equation of motion in molecular dynamic simulation are the *Verlet algorithm* [45] and *Predictor-corrector algorithm* [46].

1.3.8.3 The Verlet algorithm

The Verlet algorithm uses the positions and accelerations at time *t* and positions from the previous step, $\mathrm{r}(t-\Delta t)$, to calculate the new position at $t+\Delta t$, $\mathrm{r}(t+\Delta t)$. The following relationships between these quantities and the velocities at time *t* would be of the form

$$\mathrm{r}(t+\Delta t) = \mathrm{r}(t) + \Delta t\mathrm{v}(t) + \frac{1}{2}\Delta t^2\mathrm{a}(t) + \cdots, \tag{1.47}$$

$$\mathrm{r}(t-\Delta t) = \mathrm{r}(t) - \Delta t\mathrm{v}(t) + \frac{1}{2}\Delta t^2\mathrm{a}(t) - \cdots. \tag{1.48}$$

Combining these two equations gives

$$\mathrm{r}(t+\Delta t) = 2\mathrm{r}(t) - \mathrm{r}(t-\Delta t) + \Delta t^2\mathrm{a}(t) + \cdots. \tag{1.49}$$

In this respect, the velocities of the Verlet algorithm do not explicitly appear in the equations. However, the velocities can be calculated in many ways such as dividing the difference in positions at time $t+\Delta t$ and $t-\Delta t$ by $2\Delta t$ as

$$\mathrm{v}(t) = \left[\mathrm{r}(t+\Delta t) - \mathrm{r}(\mathrm{r}-\Delta t)\right]/2\Delta t. \tag{1.50}$$

Alternatively, the velocities can be obtained at the half-step ($t + \frac{1}{2}\Delta t$) as

$$\mathrm{v}(t + \frac{1}{2}\Delta t) = \left[\mathrm{r}(t + \Delta t) - \mathrm{r}(t)\right]/\Delta t. \tag{1.51}$$

The deficiency of Verlet algorithm is the difficulty in calculating the velocities, since these quantities cannot be obtained until the positions are computed at the next step. On the other hand, it is not a self-starting algorithm. For example, at t = 0 there is only one set of positions and it needs to know positions at $t - \Delta t$, which can be obtained by the Taylor series as

$$\mathrm{r}(-\Delta t) = \mathrm{r}(0) - \Delta t\mathrm{v}(0) - \Delta t\mathrm{v}(0). \tag{1.52}$$

The Verlet algorithm has been developed to the *leap-frog* algorithm [47], in which the positions and velocities can be written in the forms of

$$\mathrm{r}(t + \Delta t) = \mathrm{r}(t) + \Delta t\mathrm{v}(t + \frac{1}{2}\Delta t), \tag{1.53}$$

$$\mathrm{v}(t + \frac{1}{2}\Delta t) = \mathrm{v}(t - \frac{1}{2}\Delta t) + \Delta t\mathrm{a}(t). \tag{1.54}$$

The leap-frog algorithm starts with the velocities $\mathrm{v}(t + \frac{1}{2}\Delta t)$ that calculated from the velocities at time $t - \frac{1}{2}\Delta t$ and the accelerations at time t. Then, the positions $\mathrm{r}(t + \Delta t)$ are computed by the velocities that calculated together with the position at time t, r(t). The velocities at time t can be calculated from

$$\mathrm{v}(t) = \frac{1}{2}\left[\mathrm{v}(t + \frac{1}{2}\Delta t) + \mathrm{v}(t - \frac{1}{2}\Delta t)\right]. \tag{1.55}$$

In this respect, the velocities leap-frog over the positions to give their values at $t+\frac{1}{2}\Delta t$ (hence the name). Then, the positions leap-frog over the velocities to give their new values at $t+\Delta t$, ready for the velocities at $t+\frac{3}{2}\Delta t$ and so on.

With regard to the leap-frog method, however, some deficiencies are still remain, *i.e.*, this algorithm cannot calculate the positions and velocities at the same time. On the other hand, the kinetic energy contribution cannot be calculated and included into the total energy at the same time (unlike for the calculations of positions, velocities and accelerations). An alternative approach is to use the *velocity Verlet method* [48] in which the relationship between the positions and velocities can be expressed as

$$\mathrm{r}(t+\Delta t)=\mathrm{r}(t)+\Delta t\mathrm{v}(t)+\frac{1}{2}\Delta t^{2}\mathrm{a}(t), \tag{1.56}$$

$$\mathrm{v}(t+\Delta t)=\mathrm{v}(t)+\frac{1}{2}\Delta t\left[\mathrm{a}(t)+\mathrm{a}(t+\Delta t)\right]. \tag{1.57}$$

1.3.8.4 Periodic Boundary Conditions

One of the common problems found in computer simulations is the boundary effects or surface effects. This problem can be solved by using periodic boundary conditions. By this scheme, particles in the box are replicated in all directions to give a periodic array (see Figure 1.5).

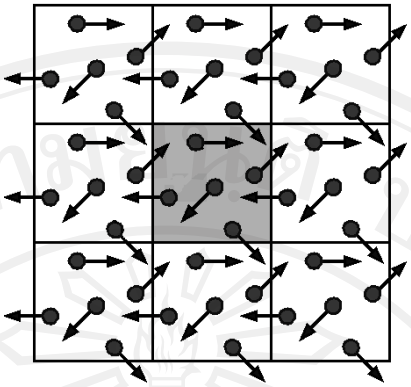

Figure 1.5 Periodic boundary conditions in two dimensions

The main point of periodic boundary conditions is the coordinates of the particles in the image boxes can be computed by adding or subtracting integral multiples of the box sides. If a particle leaves the box during the simulation, it is replaced by an image particle that enters from the opposite side in the same time, as illustrated in Figure 1.5. Therefore, the number of particles within the central box remains constant.

1.3.9 Properties calculations

1.3.9.1 Radial distribution function (RDF)

The interaction at the molecular level was investigated via the radial distribution function or RDF. The normalized RDF ($g_{AB}(r)$) is defined here as the spherically averaged distribution of inter-atomic vector lengths between two species A and B, totaling N_A and N_B in a unit cell of volume v :

$$g_{AB}(r) = \frac{N_{AB}(r)v}{4\pi r^2 dr N_A N_B} \tag{1.58}$$

where $N_{AB}(r)$ is the normalized RDF [25,31]. The cut-off radius was set to the linear dimensions of the unit cell in order to exclude self-terms.

1.3.9.2 Diffusion efficiency

1.3.9.2.1 Mean square displacement (MSD)

The diffusion of the atomic species was examined by calculating a self-diffusion coefficient from their mean-squared displacement (MSD) during the course of a simulation. This formulation is known as the Green-Kubo formulas, the results of linear response theory in statistical mechanics. To illustrate the main features of the Green-Kubo formalism we will treat explicitly the most straightforward case, that of diffusion. The MSD can be calculated by following equation

$$MSD = < \left[R(t) - R(0) \right]^2 > \tag{1.59}$$

where t is time at that calculating. R(t) and R(0) are the position at that time and the initial position by sequence [25,31].

1.3.9.2.2 Diffusion coefficient

The representative of particles translational mobilitywas analyzed in term of the diffusion coefficient (D). It can be calculated from the long time behavior of the MSD of the atom using the Einstein relation as equation

$$D = \frac{1}{6}\left[\frac{< \left[\underline{R}(t) - \underline{R}(0)\right]^2}{t}\right]_{t\to\infty} \tag{1.60}$$

where $\left[R(t) - R(0)\right]^2$ and t are MSD term and time respectively [25,31].

1.4 Aims of this research

To understand the interaction and microscopic properties of polymer electrolyte fuel cell and catalyst modifications, adding of Krytox silica composite materials in Nafion membrane, ion bombardments on Nafion membrane, nitrogen and iron plasmas sputtering on carbon, and application of imidazole-based water-free proton conducting polymer, using by molecular simulations.

References

[1] Smitha, B.; Sridhar, S.; Khan, A.A. *Journal of Membrane Science* **2005**, *259*, 10-26.

[2] Wang, Y.; Chen K. S.; Mishler, J.; Cho, S.C.; Adroher, X.C. *Applied Energy* **2011**, 88, 981-1007.

[3] Rabat, H.; Brault, P. *Fuel Cells* **2008**, *8*, 81-86.

[4] Kundu, S.; Simon, L.C.; Fowler, M.; Seabra, G. *Polymer* **2005**, *46*, 11707-11715.

[5] Prasanna, M.; Cho, E.A.; Kim, H.-J.; Lim, T.-H.; Oh, I.-H.; Hong, S. *Journal of Power Sources* 2006, 160, 90-96.

[6] http://www.bloggang.com/viewdiary.php?id=wing41&group=1&month=07-2007&date=12 (Available: June 24, 2011)

[7] Starkweather, H.W. Jr. *Macromolecules* **1982**, *15*, 320-323.

[8] Corti, H.R.; Nores-Pondal, F.; Buera, M.P. *Journal of Power Sources* **2006**, *161*, 799-805.

[9] Paddison, S.J.; Zawodzinski, T.A.Jr. *Solid State Ionics* **1998**, *113-115*, 333-340.

[10] Silva, R.F.; De Francesco, M.; Pozio, A. *Journal of Power Sources* **2004**, *134*, 18-26.

[11] Honma, I.; Nomurab, S.; Nakajima, H. *Journal of Membrane Science* **2001,** 185, 83-94

[12] Honmaa, I.; Nakajimaa, H.; Nishikawab, O.; Sugimotob, T.; Nomura, S. *Solid State Ionics* **2003**, *162*, 237-245.

[13] Gosalawit, R.; Chirachanchai, S.; Manuspiya, H.; Traversa E. *Catalysis Today* **2006**, *118*, 259-265.

[14] Gosalawit, R.; Chirachanchai, S.; Shishatskiy, S.; Nunes, S.P. *Solid State Ionics* **2007**, *178*, 1627-1635.

[15] Ye, G.; Hayden, C.A.; Goward, G.R. *Macromolecules* **2007**, *40*, 1529-1537.

[16] Kreuer, K.D.; Fuchs, A.; Ise, M.; Spaeth, M.; Maier, J. *Electrochimica Acta* **1998**, *43*, 1281-1288.

[17] Herz, H.G.; Kreuer, K.D.; Maier, J.; Scharfenberger, G.; Schuster, M.F.H.; Meyer, W. H. *Electrochimica Acta* **2003**, *48*, 2165-2171.

[18] Cho, S.A.; Cho, E.A.; Oh, I.H.; Kim, H.-J.; Ha, H.Y.; Hong, S.-A.; Ju, J.B. *Journal of Power Sources* **2006,** *155*, 286-290.

[19] Wang, B. *Journal of Power Sources* **2005**, *152*, 1-15.

[20] Bezerra, C.W.B.; Zhang, L.; Lee, K.; Liu, H.; Marques, A.L.B.; Marques, E.; Wang, H.; Zhang, J. *Electrochimica Acta*, **2008**, *53*, 4937-4951.

[21] Zhang, L.; Zhang, J.; Wilkinson, D.P.; Wang, H. *Journal of Power Sources* **2006**, *156*, 171-182.

[22] Charreteur, S.; Ruggeri, S.; Jaouen, F.; Dodelet, J-P. *Electrochimica Acta* **2008**, *53*, 2925-2938.

[23] Charreteur, F.; Jaouen, F.; Ruggeri, S.; Dodelet, J-P. *Electrochimica Acta* **2008**, *53*, 6881-6889.

[24] Paddison, S. .; Zawodzinski, T.A. Jr. *Solid State Ionics* **1998**, *113–115*, 333-340.

[25] Elliott, J.A.; Hanna, S.; Elliott, A.M.S.; Cooley, G.E. *Physical Chemistry Chemical Physics* **1999**, *1*, 4855-4863.

[26] Spencer, J.B.; Lundgen, J.O. ; *Acta Crystallographica* **1973**, *B29*, 1923-1928.

[27] Eikerling, M.; Paddison, S.J.; Pratt, L. R.; Zawodzinski, T.A.Jr. *Chemical Physics Letters* **2003**, *368*, 108-114.

[28] Seeliger, D.; Hartnig, C.; Spohr, E. *Electrochimica Acta* **2005**, *50*, 4234-4240.

[29] Joseph C. Fogarty, Hasan Metin Aktulga, Ananth Y. Grama, Adri C. T. van Duin, Sagar A. Pandit *The Journal of Chemical Physics* **2010**, *132*, 174704-1 – 174704-9.

[30] Kreuer, K.D.; Fuchs, A.; Ise, M.; Spaeth, M.; Maier, J. *Electrochimica Acta* **1998**, *43*, 1281-1288.

[31] Herz, H.G.; Kreuer, K.D.; Maier, J.; Scharfenberger, G.; Schuster, M.F.H.; Meyer, W.H. *Electrochimica Acta* **2003**, *48*, 2165-2171.

[32] Fekete, Z.A.; Wilusz, E.; Karasz, F.E. J*ournal of Polymer Science: Part B: Polymer Physics* **2004**, *42*, 1343-1350.

[33] Végh, J.J.; Nest, D.; Graves, D.B.; Bruce, R.; Engelmann, S.; Kwon, T.; Phaneuf, R.J. Oehrlein, G.S.; Long, B.K.; Willson, C.G. *Applied Physics Letters* **2007**, *91*, 233113-1,-3.

[34] Y-T. Su, Shan, T-R.; Sinnott, S.B.; *Nuclear Instruments and Methods in Physics Research Section B: Beam Interactions with Materials and Atoms* **2009**, *267*, 2525-2531.

[35] Ngaojampa, C.; Nimmanpipug, P.; Yu, L.; Anuntalabhochai, S.; Lee, V.S. *Journal of Molecular Graphics and Modelling* **2010**, *28*, 533-539.

[36] Schrödinger, E. *Quantisierung als Eigenwertproblem. Annalen der Physik* **1926**, *79*, 361-376.

[37] Slater, J.C. *Physical Review* **1929**, *34*, 1293-1322.

[38] Boys, S.F. *Proceedings of the Royal Society of London Series A* **1950**, *200*, 542-554.

[39] Kohn, W.; Sham, L.J.; *Physical Review* **1965**, *140*, A1133-A1138.

[40] Becke, A.D. *The Journal of Chemical Physics* **1986**, *84*, 4524-4529.

[41] Becke, A.D. *Physical Review A* **1988**, *38*, 3098-3100.

[42] Lee, C.; Yang, W.; Parr, R.G. *Physical Review B* **1988**, *37*, 785-789.

[43] Martin, M.G. Fluid Phase Equilibria **2006**, *248*, 50-55.

[44] Sun, H. *Journal of Physical Chemistry B* **1998**, *102*, 7338-7364.

[45] Verlet, L. *Physical Review* **1967**, *159*, 98-103.

[46] Gear, C.W. "Numerical initial value problems in ordinary differential equations" Englewood Cliffs, NJ: Prentice Hall. **1971**.

[47] Hockney, R.W. *Methods in Computational Physics* **1970**, *9*, 136-211.

[48] Verlet, L. *Physical Review* **1967**, *159*, 98-103.